

Some new IIB group complexes of an imidazolidine ligand: Synthesis, spectral characterization, electrochemical, thermal and antimicrobial properties

MORTEZA MONTAZEROZOHORI^{a,*}, SAYED ALIREZA MUSAVI^a, ASGHAR NAGHIHA^b and SOMAYEH VEYSEH^c

^aDepartment of Chemistry, Yasouj University, Yasouj 75918-74831, Iran

^bDepartment of Animal Sciences, Faculty of Agriculture, Yasouj University, Yasouj 75918-74831, Iran

^cApplied Geological Research Center of Iran, No 7, Sarbazane Gomnam Blvd, Samad Naghdi 31746-74841, Iran

e-mail: mmzohori@mail.yu.ac.ir; mmzohory@yahoo.com

MS received 24 June 2013; revised 28 October 2013; accepted 5 November 2013

Abstract. An imidazolidine Schiff base ligand, (E)-N-(4-nitrobenzylidene)-2-(2-(4-nitrophenyl) imidazolidine-1-yl) ethaneamine (L) has been synthesized by a condensation reaction between N'-(2-aminoethyl)-ethane-1,2-diamine and 4-nitrobenzaldehyde in 1:2 ratio and then characterized by physical and spectral data. Some new complexes with general formula of MLX₂ (wherein M is Zn(II), Cd(II) and Hg(II) and X is chloride, bromide and/or iodide) have been prepared and characterized by physical and spectroscopic studies such as elemental analysis, molar conductance measurements, FT-IR, ¹H and ¹³C NMR and UV-Visible electronic spectra. The spectral data indicate that the ligand is coordinated to zinc(II) as a bidentate ligand in imidazolidine form but it binds to other metal salts as bis-imine tridentate ligand. Furthermore, cyclic voltammetry technique was applied for recording the electrochemical behaviour of the ligand and its complexes. Cyclic voltamogram of the ligand showed that it is reduced at four cathodic potentials and then oxidized only in two anodic potentials in reverse direction. The electrochemical behaviour of ligand is affected by coordination. Thermal analysis of ligand and its complexes revealed that they are decomposed via 3-4 thermal steps. Moreover, some activation thermodynamic parameters such as A, E*, ΔH*, ΔS* and ΔG* were calculated based on TG/DTA plots using Coats-Redfern relation. The Schiff base ligand and its complexes have also been tested *in vitro* to evaluate their antimicrobial activities.

Keywords. Schiff base; spectroscopic; cyclic voltammetry; antibacterial; antifungal; thermogravimetry.

1. Introduction

The wide variety of possible structures for the Schiff base ligands depending upon the parent aldehydes and amines has resulted in the fast development of the chemistry of them and their complexes. Schiff base ligands as a highlighted class of organic compounds generally contain O and N donor atoms that are used for coordination to the metal ions.¹⁻⁶ In recent years, the Schiff base complexes have been found as one important group of the coordination compounds due to their valuable biochemical, analytical and antimicrobial properties.⁷⁻¹⁰ The Schiff base complexes are also applied as catalysts for a broad range of organic conversion including epoxidation of olefins, decarboxylation of arylacetic acids, hydroxylation of alkanes, polymerization of lactides and asymmetric ring opening of

epoxides.¹¹⁻¹⁵ Furthermore, many biological properties, such as DNA cleavage activity,¹⁶ biomimetic enzyme models,¹⁷⁻¹⁹ tumour growth inhibitors, antiviral, anti-HIV, antifungal and antibacterial activities²⁰⁻²⁴ have also been reported for these type of compounds. A literature survey indicates that though many reports exist on the Schiff bases, their complexes and biological applications but the synthesis and investigation of some properties such as electrochemical, thermal and biological behaviour of N₂ and N₃ donor Schiff bases and their IIB group element complexes are scanty.

In continuation of our previous studies on transition metal Schiff base complexes,²⁵⁻³⁰ here we report the synthesis and spectral characterization of a new series of MLX₂ complexes in which M is Zn(II), Cd(II) and Hg(II); X is Cl⁻, Br⁻, I⁻ and L is Schiff base ligand, (E)-N-(4-nitrobenzylidene)-2-(2-(4-nitrophenyl)imidazolidin-1-yl) ethaneamine. Furthermore,

*For correspondence

the electrochemical, antibacterial, antifungal and thermal behaviour of all compounds were investigated.

2. Experimental

2.1 Materials and methods

All solvents, *N'*-(2-aminoethyl)-ethane-1,2-diamine, 4-nitrobenzaldehyde, zinc, cadmium and mercury salts and other chemicals were provided from Aldrich and/or Merck chemical companies and used without any further purification. For biological tests, the solid medium of nutrient agar (Merck, Germany) was used for preparing the nutrient plates while Mueller Hinton broth (Scharlab) was applied as the liquid culture media. Sabouraud dextrose agar (Oxoid, Hampshire, England) was used as solid media for preparing the plates in antifungal studies. The *Escherichia coli* (ATCC 25922), *Pseudomonas aeruginosa* (ATCC 9027), *Staphylococcus aureus* (ATCC 6538) and *Bacillus subtilis* (ATCC 6633) were used as Gram-negative or positive bacterial strains in antibacterial activity evaluations. The FT-IR spectra of compounds were recorded on the FT/IR-JASCO-680 model in the range of 400–4000 cm^{-1} using KBr disks. Elemental analysis (C, N and H) was carried out by a CHNS-932(Leico) elemental analyzer. UV-Visible spectra of compounds were recorded by a JASCO-V570 spectrometer in the range of 200–800 nm in DMF solution. ^1H and ^{13}C NMR spectra were obtained by use of a Bruker DPX FT-NMR spectrometer at 400 MHz in DMSO- d_6 and/or CDCl_3 solvents using TMS as internal standard. Molar conductivities of the Schiff base ligand and its metal complexes were measured in DMF solution (1.0×10^{-3} M) by means of a Metrohm 712 conductometer at room temperature. The melting points or decomposition temperature ($^{\circ}\text{C}$) of the ligand and its complexes were recorded by a Kruss instrument. Thermogravimetric analyses of the compounds have been studied by use of STA 1500, Rheo Metric Scientific instrument in the range of room temperature to 600°C . Cyclic voltammetric (CV) measurements were performed using a three-electrode configuration cell connected to Sama 500 (electroanalysis system) equipped with glassy carbon as working electrode, Pt-disk as an auxiliary electrode and a silver wire as the reference electrode. 50 mL of sample solutions (10^{-3} M) in acetonitrile as well as (*n*-Bu) $_4$ NPF $_6$ (TBAHFP) (10^{-3} M) as supporting electrolyte were used for the CV record under argon atmosphere. A potential window of -2.0 to 0.5 V with a scan rate of 0.1 V s^{-1} was considered for electrochemical investigation.

2.2 Synthesis of (*E*)-*N*-(4-nitrobenzylidene)-2-(2-(4-nitrophenyl)imidazolidine-1-yl) ethaneamine as an imidazolidine Schiff base ligand

A solution of 4-nitrobenzaldehyde (0.302 g, 2 mmol) in methanol (20 mL) was added drop-wise to methanolic solution of *N'*-(2-aminoethyl)-ethane-1,2-diamine (0.103 g, 1 mmol) (10 mL) at room temperature and then the reaction mixture was vigorously stirred. After 3 h, the ligand as a cream precipitate was filtered and washed twice with cooled methanol and then dried on the vacuum apparatus. Some important FT/IR, UV-visible, ^1H NMR and ^{13}C NMR data are listed in below:

IR(KBr, cm^{-1}): 3434(m), 3209(m), 3101(w), 3071(w), 2941(w), 2886(w), 2848(w), 1645(s), 1601(s), 1518(vs), 1346(vs), 1293(w), 1106(w), 1065(w), 1013(w), 943(w), 851(s), 830(m), 749(s), 692(s), 462(w). **UV-Vis** [(DMF), λ (nm) (ϵ , $\text{M}^{-1} \text{cm}^{-1}$): 278(16991). ^1H NMR (CDCl_3 , ppm): 8.33(s, 1H), 8.30(d, 2H, $J = 8.76$ Hz), 8.18(d, 2H, $J = 8.76$ Hz), 7.88(d, 2H, $J = 8.80$ Hz), 7.69(d, 2H, $J = 8.60$ Hz), 4.40(s, 1H), 3.76–2.61(m, 8 $\text{H}_{\text{ethylenic}}$ and H_{NH}). ^{13}C NMR (CDCl_3 , ppm): 159.56, 148.56, 141.44, 129.98, 129.82, 128.72, 123.98, 123.72, 82.37, 61.10, 53.51, 53.46, 45.30.

2.3 Synthesis of MLX_2 complexes ($M = \text{Zn(II)}$, Cd(II) and Hg(II) and $X = \text{Cl}^-$, Br^- , I^-)

Imidazolidine Schiff base ligand (0.369 g, 1 mmol) was dissolved in 20 mL of absolute ethanol and then gradually added to methanolic solution of chloride, bromide and/or iodide salts of zinc (II), cadmium (II) and mercury (II) (1 mmol) and the mixture was continuously stirred at room temperature. The resultant precipitates were filtered off and washed with cooled ethanol and then recrystallized from dichloromethane/ethanol mixture solvent (1:1) and finally dried on the vacuum apparatus. Some important FT/IR, UV-visible, ^1H NMR and ^{13}C NMR data are listed in below:

[ZnLCl $_2$]. **IR**(KBr, cm^{-1}): 3500(m), 3253(s), 3103(w), 3068(w), 2957(w), 2935(w), 2852(w), 1649(s), 1602(s), 1522(vs), 1348(vs), 1218(w), 1106(w), 1064(w), 1018(w), 916(w), 855(s), 832(s), 747(s), 693(s), 584(w), 492(w). **UV-Vis** [(DMF), λ (nm) (ϵ , $\text{M}^{-1} \text{cm}^{-1}$): 279(20096). ^1H NMR (DMSO- d_6 , ppm): 8.43(s, 1H), 8.30(d, 2H, $J = 8.76$ Hz), 8.11(d, 2H, $J = 8.72$ Hz), 7.94(d, 2H, $J = 8.88$ Hz), 7.69(d, 2H, $J = 8.64$ Hz), 4.41(s, 1H), 3.90–2.50(m, 8 $\text{H}_{\text{ethylenic}}$ and H_{NH}). ^{13}C NMR (DMSO- d_6 , ppm): 160.03, 149.13, 148.45, 147.14, 141.59, 129.34, 128.79, 123.88, 123.05, 81.16, 59.87, 53.08, 52.68, 44.80.

[ZnLBr₂]. IR(KBr, cm⁻¹): 3445(m), 3252(s), 3102(w), 3069(w), 2954(w), 2933(w), 2850(w), 1647(s), 1602(s), 1522(vs), 1347(vs), 1217(w), 1106(w), 1083(w), 1014(w), 916(w), 854(s), 831(s), 746(s), 692(s), 582(w), 491(w). UV-Vis [(DMF), λ(nm) (ε, M⁻¹ cm⁻¹)]: 279(15586). ¹H NMR (CDCl₃, ppm): 8.70(s, 2H), 8.37(d, 4H, J = 8.80 Hz), 8.14(d, 4H, J = 8.90 Hz), 4.60(m, 4H), 3.37(m, 2H), 3.30(m, 2H), 3.10(m, 1H). ¹³C NMR (CDCl₃, ppm): 163.85, 155.65, 145.30, 130.49, 124.12, 59.62, 49.65.

[ZnLI₂]. IR(KBr, cm⁻¹): 3435(m), 3251(s), 3102(w), 3069(w), 2938(w), 2884(w), 2842(w), 1647(s), 1601(s), 1520(vs), 1438(w), 1346(vs), 1217(w), 1105(w), 1083(w), 1009(w), 934(w), 851(s), 834(m), 746(s), 692(s), 583(w), 479(w). UV-Vis [(DMF), λ(nm) (ε, M⁻¹ cm⁻¹)]: 277(17528). ¹H NMR (CDCl₃, ppm): 8.71(s, 2H), 8.37(d, 4H, J = 8.84 Hz), 8.16(d, 4H, J = 8.84 Hz), 4.06(m, 4H), 3.31(m, 4H), 3.14(m, 1H). ¹³C NMR (CDCl₃, ppm): 165.95, 151.70, 140.50, 130.79, 124.02, 58.33, 48.78.

[CdLCl₂]. IR(KBr, cm⁻¹): 3443(m), 3278(s), 3102(w), 3071(w), 2947(w), 2861(w), 2842(w), 1638(s), 1599(s), 1517(vs), 1444(w), 1347(vs), 1215(w), 1101(w), 1011(w), 941(w), 849(m), 830(m), 747(s), 690(s), 509(w), 479(w). UV-Vis [(DMF), λ(nm) (ε, M⁻¹ cm⁻¹)]: 274(14802). ¹H NMR(DMSO-d₆, ppm): 8.63(s, 2H), 8.29(d, 4H, J = 8.44 Hz), 8.08(d, 4H, J = 8.48 Hz), 3.12(bs, 4H), 2.93(m, 4H), 3.11(m, 1H). ¹³C NMR (DMSO-d₆, ppm): 161.76, 148.57, 141.21, 129.37, 123.69, 59.14, 49.11.

[CdLI₂]. IR(KBr, cm⁻¹): 3444(m), 3275(s), 3100(w), 3071(w), 2921(w), 2870(w), 1639(s), 1601(s), 1520(vs), 1423(w), 1344(vs), 1219(w), 1101(w), 1010(w), 935(w), 851(s), 837(s), 746(s), 693(s), 577(w), 491(w). UV-Vis [(DMF), λ(nm) (ε, M⁻¹ cm⁻¹)]: 275(18437). ¹H NMR(CDCl₃, ppm): 8.61(s, 2H), 8.37(d, 4H, J = 8.80 Hz), 8.17(d, 4H, J = 8.76 Hz), 4.60(bt, 2H), 3.88(bd, 2H), 3.38(m, 2H), 3.25(m, 2H), 2.59(m, 1H). ¹³C NMR (CDCl₃, ppm): 165.50, 148.15, 140.48, 131.04, 123.98, 59.73, 49.87.

[HgLI₂]. IR(KBr, cm⁻¹): 3446(m), 3215(s), 3102(w), 3074(w), 2901(w), 2881(w), 2852(w), 1639(s), 1600(s), 1519(vs), 1461(w), 1340(vs), 1217(w), 1104(w), 1008(w), 917(w), 849(m), 838(m), 747(s), 686(s), 528(w), 487(w). UV-Vis [(DMF), λ(nm) (ε, M⁻¹ cm⁻¹)]: 279(19540). ¹H NMR(CDCl₃, ppm): 8.59(s, 2H), 8.33(d, 4H, J = 8.76 Hz), 8.04(d, 4H, J = 8.80 Hz), 3.95(t, 4H), 3.25(bs, 4H), 2.49(bs, 1H). ¹³C

NMR(CDCl₃, ppm): 163.36, 149.54, 139.80, 129.86, 124.02, 59.71, 50.25.

2.4 Biological activity

Antibacterial and antifungal activities of ligand and its complexes were tested *in vitro*. For these antimicrobial investigations, two Gram-negative bacterial strains such as *Escherichia coli* and *Pseudomonas aeruginosa*; two Gram-positive bacterial strains such as *Staphylococcus aureus* and *Bacillus subtilis* and also the fungus of *Candida albicans* were selected as a typical fungal strain. The biological activities of all compounds were confirmed by determination of the minimum inhibitory concentration (MIC) values by sample dilution and disk diffusion methods. In MIC method that was used for antibacterial studies, a series of sample solutions with various concentrations (500 to 15.63 μg/mL) were prepared in DMSO in the sterile test tubes. For the bioassay of the organisms, Muller Hinton broth as basal media was added to the test tubes containing 0.1 mL of bacterium and then, these test tubes were incubated at 37°C for 24 h. For preparation of solid media in disk diffusion method, 15 mL of nutrient agar for antibacterial and sabouraud dextrose agar for antifungal studies were poured into each petri-plate. Then 0.1 mL of inoculums of the microorganism (18 h old culture) was swabbed evenly on surface of solid medium and kept for suitable adsorption for 15 min. Sterile paper disks (6 mm in diameter) were saturated with a desired solution of test compounds that has been prepared in DMSO (500 μg/mL) and then placed on the agar plates. All the plates were incubated at 37°C for 24 h and then the diameters of inhibition zones of the growth were measured by a vernier caliper.

3. Results and discussion

The (E)-N-(4-nitrobenzylidene)-2-(2-(4-nitrophenyl)imidazolidin-1-yl) ethaneamine as a new imidazolidine Schiff base ligand was prepared by a condensation reaction between 4-nitrobenzaldehyde and *N'*-(2-aminoethyl)-ethane-1, 2-diamine in 2:1 molar ratio in dry methanol. Then, some of its new complexes of zinc, cadmium and mercury halides were well-synthesized and their structures were confirmed by elemental analysis and also by FT/IR, UV-visible, ¹H and ¹³C NMR spectral data. Figure 1 illustrates the suggested structure of free ligand and its complexes. The resultant complexes (tables 1 and 2) are coloured solids and are suggested to be as non-electrolyte complexes as evidenced by their molar conductivities

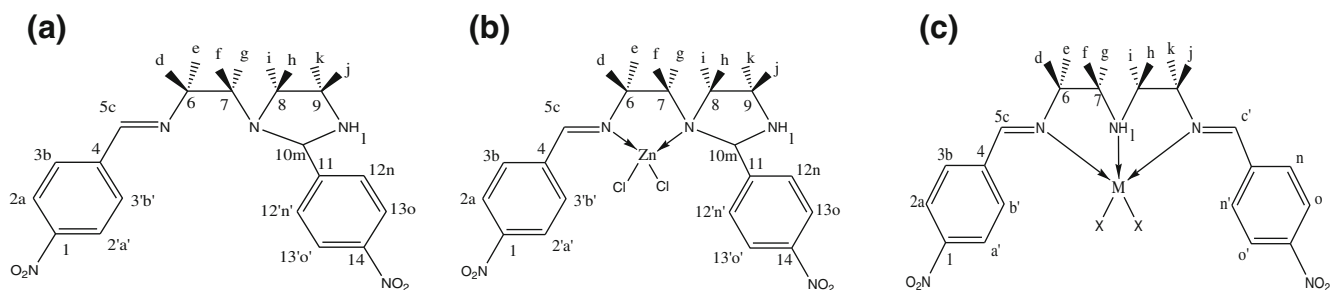


Figure 1. Proposed structure for ligand (a), ZnLCl₂ complex (b) and MLX₂ wherein M = Zn(II), X = Br⁻, I⁻; M = Cd(II), Hg(II) and X = Cl⁻, Br⁻, I⁻.

(5–28 Ω⁻¹ cm² mol⁻¹) of their solutions (10⁻³ M) in dry DMF.³¹ All compounds are very stable at room temperature in the solid state. The decomposition temperatures of the complexes were evaluated in the span of 145–241°C. Elemental analyses and other physical properties of the ligand and its complexes are summarized in table 1. The results of the elemental analyses are in a good agreement with the proposed formula.

3.1 Infra-red and electronic spectra

The characteristic frequencies of the ligand and its complexes spectra are tabulated in table 2. In the IR spectrum of ligand, the vibrational frequencies assigned to the parent amine and aldehyde compounds were not found. On the other hand, appearance of a strong absorption frequency at 1645 cm⁻¹ attributed to the vibrational stretching of the azomethine group, ν(C=N),³² indicates that the titled ligand has been successfully synthesized via a condensation reaction. This absorption frequency is smoothly shifted towards higher frequencies in zinc complexes while shifted to lower frequencies in the cadmium and mercury complexes spectra. Observation of these changes in the vibrational frequencies of azomethine groups

proves that the azomethine nitrogen atoms are coordinated to the metal ions. In the ligand spectrum, the stretching vibration of N–H is appeared as a broad peak at 3210 cm⁻¹ because of its involvement at probable hydrogen bonding. This vibration is more sharp and shifted to higher vibrational frequencies in the complexes spectra except for the complexes of entries 6 and 8.³³ The absorption frequencies of aromatic, aliphatic and azomethine CH bonds are observed at 3101 and 3071, 2941, 2886 and 2848 cm⁻¹, respectively. These absorption peaks have not considerable shift to the higher or lower frequencies in all complexes spectra. The very strong stretching vibrations at 1518 and 1346 cm⁻¹ are attributed to the asymmetric (ν_{asym}) and symmetric stretching (ν_{sym}) of –NO₂ groups that they shift a few wavenumbers to lower or higher frequencies in the complexes spectra. One of the important absorption frequencies in the complexes spectra confirming their synthesis is the vibrational frequency of M–N bond that appeared at the range of 530–584 cm⁻¹ in the complexes spectra.^{34,35} This characteristic absorption peak is not observed in the ligand spectrum (table 2).

Electronic spectra of the ligand and its complexes were recorded in DMF at room temperature and their spectral data including the λ_{max} values are tabulated

Table 1. Analytical and physical data of the imidazolidine Schiff base ligand and its zinc (II), cadmium (II) and mercury (II) complexes.

Compound	Colour	Melting point (dec.)	Yield (%)	Found (calcd.) (%)			Λ _M (cm ² Ω ⁻¹ M ⁻¹)
				C	N	H	
1 Ligand	Cream	108*	68	58.3 (58.53)	18.8 (18.96)	5.1 (5.18)	5
2 ZnLCl ₂	Cream	224	75	42.3 (42.75)	13.5 (13.85)	3.4 (3.79)	10
3 ZnLBr ₂	Cream	235	76	36.3 (36.36)	11.7 (11.78)	3.1 (3.22)	15
4 ZnLI ₂	Cream	241	80	31.2 (31.40)	10.3 (10.17)	2.5 (2.78)	19
5 CdLCl ₂	Cream	220	72	38.9 (39.12)	12.8 (12.67)	3.2 (3.47)	18
6 CdLI ₂	Cream	229	85	29.2 (29.39)	9.5 (9.52)	2.4 (2.60)	28
7 HgLI ₂	Cream	145	80	26.1 (26.24)	8.4 (8.50)	2.2 (2.32)	13

*melting point

Table 2. Vibrational (cm^{-1}) and electronic (nm) spectral data of the imidazolidine Schiff base ligand and its complexes.

Compound	ν_{NH}	$\nu_{\text{CH}_{\text{arom}}}$	$\nu_{\text{CH}_{\text{aliph}}}$	$\nu_{\text{CH}_{\text{imin}}}$	$\nu_{\text{C}=\text{N}}$	$\nu_{\text{C}=\text{C}}$	$\nu(-\text{NO}_2)$	$\nu_{\text{M}-\text{N}}$	λ_{max}
1 Ligand	3210	3101, 3071	2941	2886, 2848	1645	1601	1518, 1346	–	278
2 ZnLCl_2	3253	3103, 3068	2957, 2935	2852	1649	1602	1522, 1348	584	279
3 ZnLBr_2	3252	3102, 3069	2954, 2933	2850	1647	1602	1522, 1347	582	279
4 ZnLI_2	3251	3102, 3069	2938	2884, 2842	1647	1601	1520, 1346	583	277
5 CdLCl_2	3278	3102, 3071	2947	2861, 2842	1638	1599	1517, 1347	581	274
6 CdLI_2	3275	3100, 3071	2921	2870	1639	1601	1520, 1344	577	275
7 HgLI_2	3214	3102, 3074	2901	2881, 2852	1639	1600	1519, 1340	571	279

in table 2. In the UV-visible spectrum of the ligand, two types of internal electronic transition (IT) assigning to $\pi-\pi^*$ electron transfer of aromatic rings and $\pi-\pi^*$ transition localized within the azomethine chromophores are expected. Though it seems that these absorption bands are overlapped with each other and therefore one absorption band is appeared at 278 nm in the electronic spectrum of the ligand. This absorption band has not considerably changed in the electronic spectra of the complexes. Electronic configuration of IIB transition metal ion is d^{10} and therefore the $d-d$ electronic transition are not expected for them. In the electronic spectra of the titled complexes, the bands of charge transfer transition (MLCT) were also not observed probably due to its overlap with $\pi-\pi^*$ electronic transitions of the ligand.

3.2 ^1H and ^{13}C NMR spectra

The ^1H and ^{13}C NMR spectral data of the ligand and its metal complexes have been listed in the section 2.3. The ^1H NMR of ligand, ZnLCl_2 and HgLI_2 as typical spectra are exhibited in figure 2 and other spectra are found as supplementary information (figures S1–S12). The spectral data based on figure 1 show that the structure of free ligand and coordinated one in ZnLCl_2 complex are not symmetric. Existence of an imidazolidine ring in the structure of ligand both in free form and in ZnLCl_2 complex is well-confirmed by a signal appeared at 4.40 and 4.41 ppm assigned to imidazolidine C–H and also by a signal at 82.37 and 81.16 ppm attributed to C_{10} of imidazolidine ring in ^1H and ^{13}C NMR spectra of ligand and its ZnLCl_2 complex, respectively.³⁶ These signals are not observed at the ^1H and ^{13}C NMR spectra of other Schiff base complexes. According to ^1H NMR spectrum of ligand, the signal of proton resonance of azomethine group (H_c) as a characteristic group of Schiff base compound is appeared at 8.33 ppm as a singlet peak.³⁷ Due to binding of the azomethine nitrogen to metal centres, the azomethine proton is more deshielded so that its signal shifts to downfield region in the complexes spectra.

In the spectra of the ligand and ZnLCl_2 complex, the signal of H_{NH} is overlapped by the signals of ethylenic hydrogens and appeared at the range of 2.6–2.78 ppm and 3.2 ppm, respectively.³⁶ In the ^1H NMR spectra of other complexes, this signal was observed in the range of 2.49–3.14 ppm because of the structural change of ligand in other complexes with respect to free ligand and ZnLCl_2 complex. The hydrogens of aromatic rings in the ^1H NMR spectrum of ligand were appeared in the range of 7.69 to 8.30 ppm; H_a and a' protons were found at 8.30 ppm as doublet signal with $J = 8.76$ Hz due to coupling with hydrogens of H_b and b' . Protons of H_o and o' were appeared at 8.18 ppm as a doublet peak due to coupling with hydrogens of H_n and n' . Two doublet peaks at 7.88 and 7.69 ppm with $J = 8.8$ Hz and $J = 8.6$ Hz were assigned to H_b and b' and H_n and n' , respectively. The signals of the ethylenic hydrogens were appeared at 2.61–3.76 ppm range as eight individual multiplet peaks due to formation of imidazolidine ring leading to the asymmetrical character in ligand structure. In the ^1H NMR spectra of the complexes, the signals of aromatic ring hydrogens were observed at 7.69–8.37 ppm and the signals of ethylenic hydrogens were appeared at 2.50–4.60 ppm range. ^1H NMR spectra of the complexes showed the signals of H_a and a' and H_o and o' as doublet peaks in the range of 8.29–8.37 ppm except for entry 2. The same pattern was observed for H_b and b' and H_n and n' at 8.04–8.17 ppm. The ethylenic hydrogens of $\text{H}_{e,d,j,k}$ were found as a multiplet peaks at 3.12–4.60 ppm range. For the complex of entry 6, H_d and j and H_e and k showed different chemical shifts such that their peaks were appeared at 4.04 ppm and 3.88 ppm as a broad triplet and doublet, respectively. The ^1H NMR spectra of entries 4, 5 and 7 included multiplet peaks at 2.93–3.31 ppm range for H_f, g, h, i . In the complexes spectra of entries 3 and 6, the signals of H_f and h and H_g and i were observed at 3.37–3.38 ppm and 3.25–3.30 ppm as multiplet peaks, respectively. In some cases, it seems that the chemical shifts of ethylenic hydrogens are affected by the spatial position of H_{NH} in the complexes structures and therefore are appeared at different chemical shifts with respect to

TMS. The ^{13}C NMR spectrum of the ligand showed the azomethine carbon (C_5) resonance as functional group at 159.56 ppm. This peak is shifted to 160.03–165.95 ppm in its complexes suggesting well-coordination of the azomethine nitrogens to metal ions. In the ^{13}C NMR spectrum of the ligand, the resonance signals of aromatic carbons are suggested to be appeared at 148.56($\text{C}_{1,14}$), 141.44($\text{C}_{4,11}$), 129.98(C_{12}), 129.82($\text{C}_{12'}$), 128.72($\text{C}_{3,3'}$), 123.98($\text{C}_{2,2'}$), 123.72($\text{C}_{13,13'}$); imidazolidine carbon(C_{10}) is found at 82.37 ppm and the ethylenic carbons resonance are observed as four individual peaks at 61.10(C_8), 53.51(C_6), 53.46(C_9) and 45.30(C_7) ppm. In the ^{13}C NMR spectrum of ZnLCl_2 complex containing the retained structure of ligand, the peaks of aromatic ring carbons and imidazolidine carbon may be assigned as 149.13(C_1), 148.45(C_{14}), 147.14(C_4), 141.59(C_{11}), 129.34($\text{C}_{12,12'}$), 128.79($\text{C}_{3,3'}$), 123.88($\text{C}_{2,2'}$), 123.05($\text{C}_{13,13'}$) and 81.16 (C_{10}) ppm, respectively. On the other hand, the ethylenic carbons signals are observed as four characteristic peaks at 59.87(C_8), 53.08(C_6), 52.68(C_9) and 44.80(C_7) ppm. In the ^{13}C NMR spectra of other complexes, seven signals of carbon resonances assigned to seven types of carbons in the symmetric structures of them are obviously observed. For these complexes, the azomethine carbon signals appeared at 161.76–165.95 ppm range show a downfield shift with respect to one in free ligand. Finally, the signals attributed to (C_1), (C_4), (C_3), (C_2), (C_6) and (C_7) are found in the ranges of 148.15–155.65, 139.80–145.30, 129.37–131.04, 123.69–124.12, 58.33–58.73 and 48.78–50.25 ppm in the complexes spectra, respectively.

3.3 Coordination mode

With regard to spectral data, it is suggested that the ligand is formed as imidazolidine Schiff base (figure 1a) not as a simple bis-azomethine ligand. This type of Schiff base ligand has been previously reported by Yue *et al.*³⁶ The titled imidazolidine Schiff base is coordinated to zinc chloride without ring opening of the imidazolidine and acts as a bidentate N_2 -ligand that along with chloride anions forms pseudo-tetrahedral geometry around the zinc ion. Coordination of the ligand to other metal salts is accompanied with imidazolidine ring opening so that the ligand is coordinated to metal centers as a tridentate bis-azomethine amine ligand such that five coordinated complexes are formed along with halide anions similar to some other previous reports.^{38,39} The change in coordination mode of the ligand may be due to electronic and steric effect of metal ion and its halide anions so that where the metal

ion is zinc and halide is chloride, the coordination of imidazolidine Schiff base ligand is possible as shown in figure 1b but when the metal ion and/or halide anions is changed to more voluminous and polarizable ones, the electronic and steric effects prevent the coordination of ligand as imidazolidine form. Therefore, imidazolidine ring of ligand is opened during the coordination of ligand as shown in figure 1c.

3.4 Thermal investigation

Thermal behaviour (TG/DTA) of the titled compounds were investigated at the heating rate of 10 ($^\circ\text{C}/\text{min}$) under nitrogen atmosphere from room temperature to 600 $^\circ\text{C}$. TG/DTA plots of the ligand, zinc and mercury iodide complexes as illustrative diagrams in figure 3. Thermal analysis data including thermal decomposition steps, mass loss (%) and thermodynamic activation parameters of each decomposition steps of the ligand and its complexes have been derived and tabulated in table 3 based on TG/DTA plots.

The TG diagrams confirm the absence of water molecules in the complex structures. The TG/DTA plots of ligand and its complexes indicate that they are decomposed in four successive thermal steps except for ZnLBr_2 that is decomposed in three thermal steps. First thermal step in the TG plots of all compounds may be assigned to thermal elimination of nitro-groups. In the next thermal steps, the ligand and its complexes lose 38.58–81.9% of total mass up to 600 $^\circ\text{C}$ attributed to other organic segments as suggested in table 3.

Moreover, the thermodynamic activation parameters of thermal decomposition steps of the ligand and its complexes including Arrhenius constant (A), activation energy (E^*), enthalpy (ΔH^*), entropy (ΔS^*) and Gibbs free energy (ΔG^*) of thermal steps were evaluated using Coats–Redfern relation based on TG plots.^{40,41} Activation parameters evaluation of the ligand and its complexes may be carried out to suggest the thermal stability of them. The resultant values showed that the activation energies (E^*) in the different steps of thermal decomposition processes are found in the range of 22.57–352.69 kJmol^{-1} indicating relatively high thermal stability of the compounds. The values of the activation entropy (ΔS^*) are evaluated as negative numbers for all thermal decomposition steps of compounds except for the first thermal steps of ligand, zinc and cadmium iodide complexes and are found in the range of $-266 - 409 \text{ Jmol}^{-1} \text{ K}^{-1}$. The negative values suggest an associated mechanism at rate determining step of thermal decomposition process similar to many reports in the literature in this matter. All evaluated ΔH^* and ΔG^* values for the compounds are positive

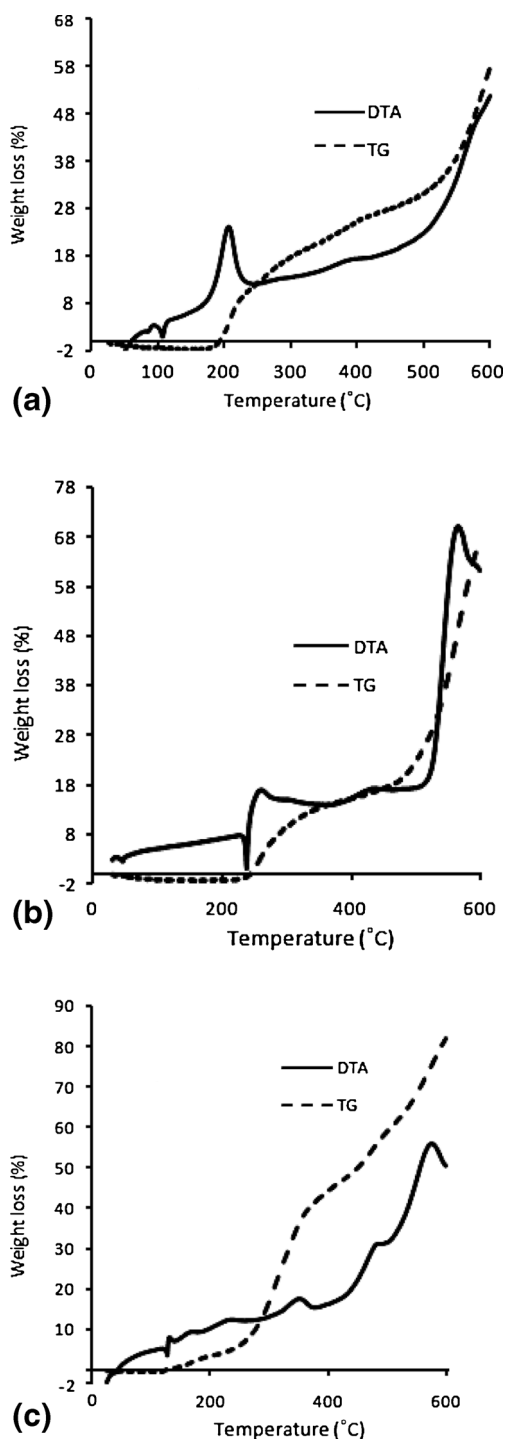


Figure 3. TG/DTA diagrams of ligand (a), zinc iodide complex (b) and mercury iodide complex (c).

numbers in the range of 17.5 to 348.53 kJmol⁻¹ and 134 to 249 kJmol⁻¹, respectively indicating endothermic character of all thermal decomposition steps.

3.5 Cyclic voltammetry

The electrochemical behaviour of the Schiff base ligand and its complexes (10⁻³ M) were studied by

cyclic voltammetry technique in the potential window of -2.00 to 0.5 V in dry acetonitrile solution containing (*n*-Bu)₄NPF₆(TBAHP) as supporting electrolyte (10⁻³ M). The cyclic voltammograms of ligand, zinc chloride and mercury iodide complexes have been illustrated in figure 4 as representative diagrams while all electrochemical data considered as potential window have been tabulated in table 4. Cyclic voltammogram of ligand showed four cathodic and two anodic potential peaks. The cathodic peaks (E_{pc}) were found at -0.81 V(I), -0.95 V(II), -1.35 V(III) and -1.64 V(IV) while two anodic peaks (E_{pa}) were appeared at -0.74 V and -0.87 V in relative to I and II cathodic potential peaks. The cathodic peaks appeared at -0.81 V and -0.95 V may be corresponded to the reduction of two different nitro-groups in the ligand structure (as shown in figure 1) to nitro-anion radicals and then to nitroso groups in one step, respectively. These reduction steps are quasi-reversibly followed (potential difference(ΔE_p) values are 0.070 V and 0.080 V, respectively) by two anodic peaks as mentioned above. The irreversible cathodic peaks appeared at -1.35 V and -1.64 V may be attributed to the reduction of the nitroso groups to the hydroxyl amine and then to amine groups, respectively.^{42,43} Based on electrochemical data in table 4, it seems that in zinc chloride and bromide complexes, the reduction of one nitro-group to nitroso group have occurred via two different steps (peaks IIa, IIb) (instead of one step observed in free ligand as mentioned above) with anodic and cathodic shifts for (I, IIa) and IIb with respect to free ligand as shown in table 4 while other reduction peaks (III and IV) are seen in a model similar to free ligand. The electrochemical behaviour of coordinated ligand in zinc iodide is similar to free ligand but with an anodic shift in its potential values. The anodic shift in potential values of ligand in zinc complexes is due to its coordination to metal centre and then induction of positive charge on ligand structure that facilitates its redox behaviour. Voltammograms of cadmium chloride and cadmium iodide complexes also show the same electrochemical behaviour as observed for the free ligand but with a cathodic shift in redox potential values confirming a well-coordination of ligand. The cathodic shift may be because of an induction of negative charge on ligand structural surface because of an efficient π -back bonding from cadmium ion as an electron-rich metal ion to ligand π^* orbitals(π^* of iminic bond(C=N)) after initial coordination.⁴⁴⁻⁴⁶ For mercury iodide complex, a electrochemical behaviour similar to coordinated ligand in the cadmium complexes is observed but the fourth reduction is not observed suggesting a high cathodic shift to out of studied potential window.

Table 3. Thermal analysis data including thermal decomposition steps, mass loss (%) and thermodynamic activation parameters of thermal steps of ligand and its complexes.

Compound	Thermal step(°C)	Mass loss(%)	Total mass loss(%)	E*(kJmol ⁻¹)	A(s ⁻¹)	ΔS*(kJmol ⁻¹)	ΔH*(kJmol ⁻¹)	ΔG*(kJmol ⁻¹)
Ligand	160–240	11.3	56.3	239.34	5.32 × 10 ²³	2.05 × 10 ²	235.39	1.38 × 10 ²
	240–340	8.3		33.66	2.99	-2.41 × 10 ²	29.08	1.62 × 10 ²
	340–470	8.5		54.42	4.61 × 10 ¹	-2.20 × 10 ²	48.84	1.96 × 10 ²
	470–600	28.2		96.25	1.99 × 10 ³	-1.90 × 10 ²	89.26	2.49 × 10 ²
ZnLBr ₂	200–310	11.04	38.58	129.66	1.95 × 10 ¹⁰	-5.26 × 10 ¹	125.33	1.53 × 10 ²
	310–430	3.04		64.66	6.16 × 10 ²	-1.98 × 10 ²	59.22	1.89 × 10 ²
	430–600	24.5		108.37	1.18 × 10 ⁴	-1.76 × 10 ²	101.39	2.49 × 10 ²
ZnLI ₂	210–285	9.04	58.13	175.70	6.75 × 10 ¹⁴	3.42 × 10 ¹	171.31	1.53 × 10 ²
	285–340	4.9		54.21	2.23 × 10 ²	-2.06 × 10 ²	49.34	1.70 × 10 ²
	340–415	3.1		31.15	8.06 × 10 ⁻¹	-2.53 × 10 ²	25.83	1.88 × 10 ²
	415–600	51.09		135.91	7.03 × 10 ⁵	-1.42 × 10 ²	128.96	2.47 × 10 ²
CdLCl ₂	180–275	13.88	46.38	94.95	1.90 × 10 ⁷	-1.10 × 10 ²	90.85	1.45 × 10 ²
	275–360	4.00		26.21	5.63 × 10 ⁻¹	-2.55 × 10 ²	21.44	1.68 × 10 ²
	360–455	3.00		100.50	3.03 × 10 ⁵	-1.47 × 10 ²	94.77	1.96 × 10 ²
	455–600	25.5		46.47	8.50 × 10 ⁻¹	-2.55 × 10 ²	39.82	2.43 × 10 ²
CdLI ₂	210–265	8.13	59.46	352.69	2.29 × 10 ³⁴	4.09 × 10 ²	348.53	1.44 × 10 ²
	265–380	8.43		22.57	1.69 × 10 ⁻¹	-2.66 × 10 ²	17.57	1.77 × 10 ²
	380–500	15.00		48.10	3.79	-2.41 × 10 ²	42.04	2.18 × 10 ²
	500–600	27.9		79.10	1.92 × 10 ²	-2.10 × 10 ²	72.22	2.46 × 10 ²
HgLI ₂	120–230	4.79	81.90	39.31	5.85 × 10 ¹	-2.15 × 10 ²	35.51	1.34 × 10 ²
	230–435	43.41		34.98	1.35	-2.49 × 10 ²	29.69	1.88 × 10 ²
	435–520	14.10		50.84	7.68	-2.36 × 10 ²	44.59	2.22 × 10 ²
	520–600	19.6		67.34	3.57 × 10 ¹	-2.24 × 10 ²	60.34	2.49 × 10 ²

Furthermore, two new reversible redox potentials are observed at mercury iodide complex voltammogram as I' and II' peaks that may be attributed to Hg(II)/(I) and Hg(I)/(0) redox pairs, respectively.

3.6 Antibacterial and antifungal activity

The Schiff base ligand and its metal complexes were tested *in vitro* for their antibacterial activities against

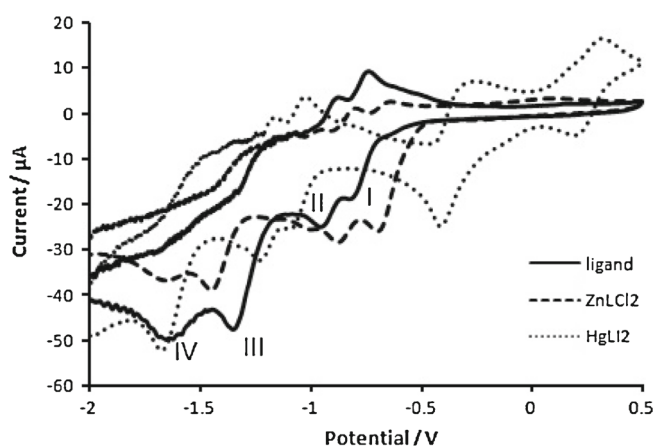


Figure 4. The cyclic voltammograms of ligand, ZnLCl₂ and HgLI₂ in dry acetonitrile.

two Gram-negative and two Gram-positive bacterial strains including *Escherichia coli*, *Pseudomonas aeruginosa*, *Staphylococcus aureus* and *Bacillus subtilis* bacteria and also for their inhibitory effects on the growth of *Candida albicans* using disc diffusion and MIC methods. The antibacterial activities of the ligand and its complexes as inhibition zone (mm) of the bacterial and fungal growth have been classified in table 5 and also depicted as column diagram in figure 5. The solutions with concentration of 500 µg/mL of Schiff base ligand and its complexes in DMSO were applied in disc diffusion technique. The effective material on each disk was estimated to be 25 µg. The MIC method was also performed for all the compounds by use of the sample solutions with 15.63, 31.25, 62.50, 125, 250, 500 µg/mL concentrations. The results showed that the synthesized complexes are more antimicrobial active as compared with their parent Schiff base ligand against the same bacteria and fungi under the same experimental conditions. An increase in the inhibitory effect of the complexes as compared with the free ligand may be discussed based on Overtone's concept and Tweedy's chelation theory.^{47,48} The cell membrane has been made from lipid layers that are permeable only for lipid-soluble materials. The antibacterial activity of

Table 4. The cyclic voltammetric data of imidazolidine Schiff base ligand and its complexes.

Compound	Peak	E_{pc} (V)	E_{pa} (V)	ΔE_p (V)
Ligand	I	-0.81	-0.74	0.070
	II	-0.95	-0.87	0.080
	III	-1.35	-	-
	IV	-1.64	-	-
ZnLCl ₂	I	-0.69	-0.64	0.050
	IIa	-0.88	-0.79	0.090
	IIb	-1.01	-0.95	0.060
	III	-1.45	-	-
	V	-1.65	-	-
ZnLBr ₂	I	-0.61	-0.51	0.100
	IIa	-0.88	-0.76	0.120
	IIb	-1.02	-0.91	0.110
	III	-1.5	-	-
	IV	-1.77	-	-
ZnLI ₂	I	-0.76	-0.67	0.090
	II	-0.89	-0.82	0.070
	III	-1.45	-	-
	IV	-1.6	-	-
CdLCl ₂	I	-0.88	-0.79	0.090
	II	-0.99	-0.94	0.050
	III	-1.45	-	-
	IV	-1.76	-	-
CdLI ₂	I	-0.92	-0.83	0.090
	II	-1.05	-0.98	0.070
	III	-1.66	-	-
	IV	-1.83	-	-
HgLI ₂	I'	0.2	0.32	0.120
	II'	-0.41	-0.29	0.120
	I	-1.09	-1.02	0.070
	II	-1.23	-1.16	0.070
	III	-1.67	-	-

a compound is depended on its liposolubility character. After coordination of organic ligand to metal centre, the polarity of the metal ion considerably is reduced due to overlap of its valence orbitals with the ligand orbitals. This leads to a decrease in positive charge of

metal ion and π -electron delocalization within whole of the ligand chelating ring that would certainly enhance the lipophilic character of the central metal ion. The increased lipophilicity character causes more diffusion of the complexes into cell membrane and blocks the

Table 5. Antibacterial and antifungal activities of 25 μ g/disk of the imidazolidine Schiff bases ligand and its complexes based on inhibition zone of the bacterial and fungal growth (mm) and their MIC values (μ g/mL).

Compound	Gram-negative bacteria				Gram-positive bacteria				<i>Candida albicans</i> zone (mm)
	<i>Escherichia coli</i>		<i>Pseudomonas aeruginosa</i>		<i>Bacillus subtilis</i>		<i>Staphylococcus aureus</i>		
	MIC (μ g/mL)	zone (mm)	MIC (μ g/mL)	zone (mm)	MIC (μ g/mL)	zone (mm)	MIC (μ g/mL)	zone (mm)	
Ligand	500	11.50	500	6.80	500	14.46	500	10.00	17.40
ZnLCl ₂	250	15.50	500	8.44	250	17.00	250	12.00	24.80
ZnLBr ₂	500	12.20	500	7.90	500	15.00	500	11.50	21.80
ZnLI ₂	250	15.20	500	8.60	500	14.80	125	16.20	18.50
CdLCl ₂	125	16.19	125	10.60	125	17.70	250	15.90	22.20
CdLI ₂	500	11.50	250	9.80	65.50	23.80	250	16.00	17.80
HgLI ₂	125	17.66	125	10.70	65.50	23.40	62.50	21.90	26.50

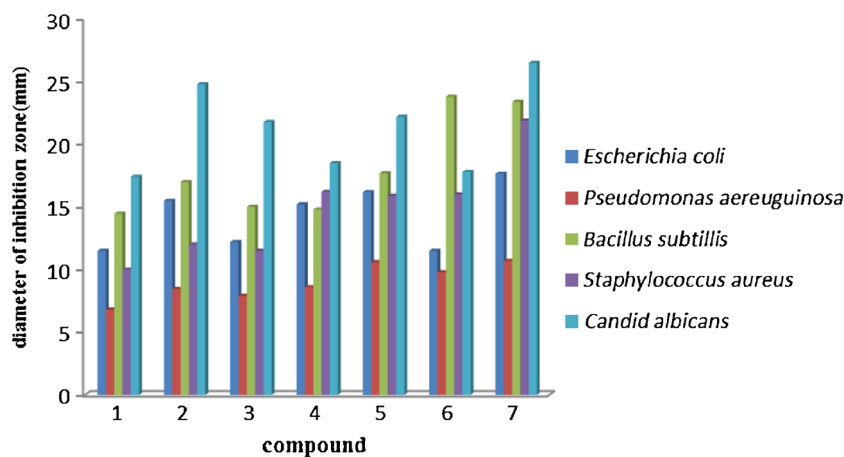


Figure 5. The inhibition zone of the growth of bacteria and fungus (mm) (the numbers refer to entries of the tables).

metal coordination sites of the enzymes in the bacteria and/or fungi structures. In the case of antibacterial studies, it was observed that HgLI_2 complex is the most active compound against *Staphylococcus aureus* with a MIC value of $62.5 \mu\text{g/mL}$. The growth of *Escherichia coli* and *Pseudomonas aeruginosa* was more efficiently inhibited by CdLCl_2 and HgLI_2 complexes (MIC = $125 \mu\text{g/mL}$) with respects to other compounds. Among the investigated compounds, HgLI_2 and CdLI_2 complexes showed higher activities against *Bacillus subtilis* with respect to others. The antifungal activities of the ligand and its complexes were checked by disc diffusion method and the results revealed that the inhibitory effect of the ligand was enhanced after its chelation to metal ions. In this investigation, it was recognized that HgLI_2 complex efficiently prevents the growth of *Candida albicans* as compared with free ligand. Finally, zinc chloride, zinc bromide, cadmium chloride, zinc and cadmium iodide were found in the next positions in the antifungal activity point of view with respect to free ligand.

4. Conclusion

In this work, the synthesis and characterization of a new imidazolidine Schiff base ligand and some new zinc, cadmium and mercury complexes are described. The spectral data confirmed that the ligand is coordinated to metal ions in two coordination modes as bidentate and/or tridentate ligand. The electrochemical investigations showed that the ligand is reduced at four cathodic potentials and then oxidized at two anodic potentials in reverse direction. After complexation, the coordinated ligand retains its redox behaviour but with anodic and/or cathodic shifts in potential peaks. In mercury complex, two new reversible redox potentials appeared that may be assigned to redox pairs of Hg(II)/(I) and

Hg(I)/(0) . TG/DTA plots of ligand and its complexes have revealed that there are no water molecules in the complex structure. Thermal analyses data of the ligand and its complex indicated that they are decomposed and lose 38.58–81.9% of total mass from the room temperature to 600°C . Finally, the antibacterial/antifungal activities of the compounds were screened against two Gram-negative and positive bacterial strains and also a fungus. All complexes have shown more antibacterial/antifungal active compounds as compared with the free ligand.

Supplementary information

Figures S1–S12 as supplementary information can be seen at www.ias.ac.in/chemsci website.

References

1. Holm R H and Oconnor M 1971 *Prog. Inorg. Chem.* **14** 241
2. Holm R H, Evert G W and Chakravorty A 1966 *Prog. Inorg. Chem.* 783
3. Coles S J, Hursthouse M B, Kelly D G, Toner A J and Walker N M 1998 *J. Chem. Soc. Dalton Trans.* **20** 3489
4. Tumer M, Koksall H, Sener M K and Serin S 1999 *Transition. Met. Chem.* **24** 414
5. Budzisz E, Keppler B K, Giester G, Wozniczka M, Kufelnicki A and Nawrot B 2004 *Eur. J. Inorg. Chem.* **22** 4412
6. Sedaghat T, Naseh M, Bruno G, Amiri Rudbari H and Motamedi H 2012 *J. Mol. Struc.* **1026** 44
7. Jimenez M, Mateo J J and Mateo R 2000 *J. Chromatogr. A* **870** 473
8. Thati B, Noble A, Creaven B S, Walsh M, McCann M, Kavanagh K, Devereux M and Egan D A 2007 *Cancer Lett.* **248** 321
9. Mohamed R R and Fekry A M 2011 *Int. J. Electrochem. Sci.* **6** 2488

10. Ravi Krishna E, Muralidhar Reddy P, Sarangapani M, Hanmanthu G, Geeta B, Shoba Rani K and Ravinder V 2012 *Spectrochim. Acta A* **97** 189
11. Montazerzohori M, Habibi M H, Zamani-Fradonbe L and Musavi S A R 2008 *Arkivoc* **xi** 238
12. Zhan J, Zhan B, Liu J, Xu W J and Wang Z 2001 *Spectrochim. Acta A* **57** 149
13. Srinivasan K and Kochi J K 1986 *J. Am. Chem. Soc.* **108** 2309
14. Jacobsen E N, Zhang W, Muci A R, Ecker J R and Deng L 1990 *J. Am. Chem. Soc.* **112** 2801
15. Jacobsen E N 2000 *Acc. Chem. Res.* **33** 421
16. Shahabadi N, Kashanian S and Darabi F 2010 *Eur. J. Med. Chem.* **45** 4239
17. Collinson S R and Fenton D E 1996 *Coord. Chem. Rev.* **148** 19
18. Santos M L P, Bagatin I A, Pereira E M and Ferreira A M C 2001 *J. Chem. Soc. Dalton Trans.* **6** 838
19. He H S, Puerta D T, Cohen S M and Rodgers K R 2005 *Inorg. Chem.* **44** 7431
20. Pandeya S N, Sriram D, Ath G and DeClecq E 1999 *Eur. J. Pharm.* **9** 25
21. Wang M, Wang L F, Li Y Z, Li Q X, Xu Z D and Qu D Q 2001 *Transition Met. Chem.* **26** 307
22. Gulerman N N, Rollas S, Erdeniz H and Kiraj M 2001 *J. Pharm. Sci.* **26** 1
23. Tarasconi P, Capacchi S, Pelosi G, Corina M, Albertini R, Bonati A, Dall'Aglio P P, Lunghi P and Pinelli S 2000 *Bioorg. Med. Chem.* **8** 154
24. Anitha C, Sheela C D, Tharmaraj P and Sumathi S 2012 *Spectrochim. Acta A* **96** 493
25. Habibi M H, Montazerzohori M, Lalegani A, Harington R W and Clegg W 2007 *Anal. Sci. X-ray Struct. Anal Online* **23** X49
26. Montazerzohori M and Musavi S A 2008 *J. Coord. Chem.* **61** 3934
27. Montazerzohori M, Joohari S and Musavi S A 2009 *J. Coord. Chem.* **62** 1282
28. Montazerzohori M and Sedighipoor M 2012 *Spectrochim. Acta Part A* **96** 70
29. Montazerzohori M, Hojjati A, Joohari S and Ebrahimi H R 2012 *Int. J. Electrochem. Sci.* **7** 11758
30. Montazerzohori M, Khani S, Tavakol H, Hojjat A and Kazemi M 2011 *Spectrochim. Acta Part A* **81** 122
31. Chan M E, Crouse K A, Tahir M I M, Rosli R, Umar-Tsafe N and Cowley A R 2008 *Polyhedron* **27** 1141
32. Chakraborty J, Thakurta S, Samanta B, Ray A, Pilet G, Batten S R, Jensen P and Mitra S 2007 *Polyhedron* **26** 5139
33. Dede B, Karipcin F and Cengiz M 2009 *J. Hazard. Mater.* **163** 1148
34. Celik C, Tumer M and Serin S 2002 *Synth. React. Inorg. Met.-Org. Chem.* **32** 1839
35. El-Tabl A S, El-Saied F A, Plass W and Al-Hakimi A N 2008 *Spectrochim. Acta Part A* **71** 90
36. Yue F, Gang L, Xiu-Mei T, Ji-De W and Wei W 2008 *Chin. J. Struct. Chem.* **27** 455
37. Basak S, Sen S, Marschner C, Baumgartner J, Batten S R, Turner D R and Mitra S 2008 *Polyhedron* **27** 1193
38. Chun-Hong L, Qiang W, Yan-Qing X and Chang-Wen H 2008 *Chin. J. Struct. Chem.* **27** 187
39. Gwaram N S, Ali H M, Khaledi H, Abdulla M A, Hamid A, Hadi A, Lin T K, Ching C L and Ooi C L 2012 *Molecules* **17** 5952
40. Soliman A A 2001 *J. Therm. Anal. Calorim.* **63** 221
41. Sen S, Talukder P, Rosair G and Mitra S 2005 *Struct. Chem.* **16** 605
42. Zeybek B, Durmus Z, Tekiner-Gülbas B, Aki-sener E, Yalcin I and Kilic E 2009 *Curr. Pharm. Anal.* **5** 21
43. Carbajo J, Bollo S, Nunez-Vergara L J, Campero A and Squella J A 2002 *J. Electroanal. Chem.* **531** 187
44. Salonen M, Saarinen H and Orama M 2003 *J. Coord. Chem.* **56** 1041
45. Banerjee S, Wu B, Lassahn P G, Janiak C and Ghosh A 2005 *Inorg. Chim. Acta* **358** 535
46. Satoh K, Takahashi Y, Suzuki T and Sawada K 1989 *J. Chem. Soc. Dalton Trans.* **7** 1259
47. Tweedy B G 1964 *Phytopathology* **55** 910
48. Searl J W, Smith R C and Wyard S J 1961 *Proc. Phys. Soc.* **78** 1174